Chapter 9

Multiple Importance Sampling

We introduce a technique called *multiple importance sampling* that can greatly increase the reliability and efficiency of Monte Carlo integration. It is based on the idea of using more than one sampling technique to evaluate a given integral, and combining the sample values in a provably good way.

Our motivation is that most numerical integration problems in computer graphics are "difficult", i.e. the integrands are discontinuous, high-dimensional, and/or singular. Given a problem of this type, we would like to design a sampling strategy that gives a low-variance estimate of the integral. This is complicated by the fact that the integrand usually depends on parameters whose values are not known at the time an integration strategy is designed (e.g. material properties, the scene geometry, etc.) It is difficult to design a sampling strategy that works reliably in this situation, since the integrand can take on a wide variety of different shapes as these parameters vary.

In this chapter, we explore the general problem of constructing low-variance estimators by combining samples from several different sampling techniques. We do not construct new sampling techniques — we assume that these are given to us. Instead, we look for better ways to combine the samples, by computing weighted combinations of the sample values. We show that there is a large class of unbiased estimators of this type, which can be parameterized by a set of weighting functions. Our goal is to find an estimator with minimum variance, by choosing these weighting functions appropriately.

A good solution to this problem turns out to be surprisingly simple. We show how to combine samples from several techniques in a way that is provably good, both theoretically and practically. This allows us to construct Monte Carlo estimators that have low variance for a broad class of integrands — we call such estimators *robust*. The significance of our methods is not that we can take several bad sampling techniques and concoct a good one out of them, but rather that we can take several potentially good techniques and combine them so that the strengths of each are preserved.

This chapter is organized as follows. We start with an extended example to motivate our variance reduction techniques (Section 9.1). Specifically, we consider the problem of computing the appearance of a glossy surface illuminated by an area light source. Next, in Section 9.2 we explain the multiple importance sampling framework. Several models for taking and combining the sampling are described, and we present theoretical results showing that these techniques are provably close to optimal (proofs may be found in Appendix 9.A). In Section 9.3, we show that these techniques work well in practice, by presenting images and numerical measurements for two specific applications: the glossy highlights problem mentioned above, and the “final gather” pass that is used in some multi-pass algorithms. Finally, Section 9.4 discusses of a number of tradeoffs and open issues related to our work.

9.1 Application: glossy highlights from area light sources

We have chosen a problem from distribution ray tracing to illustrate our techniques. Given a glossy surface illuminated by an area light source, the goal is to determine its appearance. These “glossy highlights” are commonly evaluated in one of two ways: either by sampling the light source, or sampling the BSDF. We show that each method works very well in some situations, but fails in others. Obviously, we would prefer a sampling strategy that works well all the time. Later in this chapter, we will show how multiple importance sampling can be applied to solve this problem.

9.1.1 The glossy highlights problem

Consider an area light source S that illuminates a nearby glossy surface (see Figure 9.1). The goal is to determine the appearance of this surface, i.e. to evaluate the radiance $L_{\mathrm{o}}(\mathbf{x}', \omega_{\mathrm{o}}')$

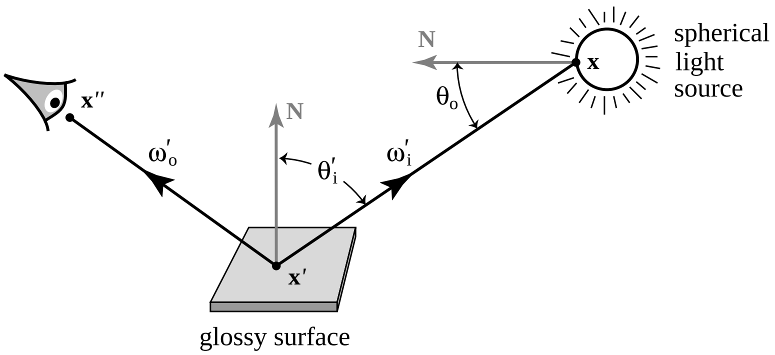

Figure 9.1: Geometry for the glossy highlights computation. The radiance for each viewing ray is obtained by integrating the light that is emitted by the source, and reflected from the glossy surface toward the eye.

that leaves the surface toward the eye. Mathematically, this is determined by the scattering equation (3.12):

$$L_\mathrm{o}(\mathbf{x}', \omega'_\mathrm{o}) \;=\; \int_{\mathcal{S}^2} f_\mathrm{s}(\mathbf{x}', \omega'_\mathrm{i} \!\rightarrow\! \omega'_\mathrm{o}) \, L_\mathrm{e,i}(\mathbf{x}', \omega'_\mathrm{i}) \, d\sigma^\perp(\omega'_\mathrm{i}) \,, \tag{9.1}$$

where $L_\mathrm{e,i}$ represents the incident radiance due to the area light source S.

We will examine a family of integration problems of this form, obtained by varying the size of the light source and the glossiness of the surface. In particular, we consider spherical light sources of varying radii, and glossy materials that have a *surface roughness parameter* (r) that determines how sharp or fuzzy the reflections are. Smooth surfaces ($r = 0$) correspond to highly polished, mirror-like reflections, while rough surfaces ($r = 1$) correspond to diffuse reflection. It is possible to simulate a variety of surface finishes by using intermediate roughness values in the range $0 < r < 1$.

9.1.2 Two sampling strategies

There are two common strategies for Monte Carlo evaluation of the scattering equation (9.1), which we call *sampling the BSDF* and *sampling the light source*. The results of these techniques are demonstrated in Figure 9.2(a) and Figure 9.2(b) respectively, over a range of different light source sizes and surface finishes. We will first describe these two strategies, and then examine why each one has high variance in some situations.

Sampling the BSDF. To sample the BSDF, an incident direction ω'_i is randomly chosen according to a predetermined density $p(\omega'_\mathrm{i})$. Normally, this density is chosen to be proportional to the BSDF (or some convenient approximation), i.e.

$$p(\omega'_\mathrm{i}) \;\propto\; f_\mathrm{s}(\mathbf{x}', \omega'_\mathrm{i} \!\rightarrow\! \omega'_\mathrm{o})\,,$$

where p is measured with respect to projected solid angle. To estimate the scattering equation (9.1), an estimate of the usual form

$$L_\mathrm{o}(\mathbf{x}', \omega'_\mathrm{o}) \;\approx\; \frac{f_\mathrm{s}(\mathbf{x}', \omega'_\mathrm{i} \!\rightarrow\! \omega'_\mathrm{o})\, L_\mathrm{e,i}(\mathbf{x}', \omega'_\mathrm{i})}{p(\omega'_\mathrm{i})}$$

is used. The emitted radiance $L_\mathrm{e,i}(\mathbf{x}', \omega'_\mathrm{i})$ is evaluated by casting a ray to find the corresponding point on the light source. Note that some rays may miss the light source S, in which case they do not contribute to the highlight calculation. The image in Figure 9.2(a) was computed using this strategy.

Sampling the light source. To explain the other strategy, we first rewrite the scattering equation as an integral over the surface of the light source:

$$L_\mathrm{o}(\mathbf{x}' \!\rightarrow\! \mathbf{x}'') \;=\; \int_{\mathcal{M}} f_\mathrm{s}(\mathbf{x} \!\rightarrow\! \mathbf{x}' \!\rightarrow\! \mathbf{x}'')\, L_\mathrm{e}(\mathbf{x} \!\rightarrow\! \mathbf{x}')\, G(\mathbf{x} \!\leftrightarrow\! \mathbf{x}')\, dA(\mathbf{x})\,. \qquad (9.2)$$

This is called the *three-point form* of the scattering equation (previously described in Section 8.1). The function G represents the change of variables from $d\sigma^\perp(\omega'_\mathrm{i})$ to $dA(\mathbf{x})$, and is given by

$$G(\mathbf{x} \!\leftrightarrow\! \mathbf{x}') \;=\; V(\mathbf{x} \!\leftrightarrow\! \mathbf{x}')\, \frac{|\cos(\theta_\mathrm{o})\; \cos(\theta'_\mathrm{i})|}{\|\mathbf{x} - \mathbf{x}'\|^2}$$

(see Figure 9.1).

The strategy of sampling the light source now proceeds as follows. First, a point $\mathbf{x}$ on the light source S is randomly chosen according to a predetermined density $p(\mathbf{x})$, and then a standard Monte Carlo estimate of the form

$$L_\mathrm{o}(\mathbf{x}' \!\rightarrow\! \mathbf{x}'') \;\approx\; \frac{L_\mathrm{e}(\mathbf{x} \!\rightarrow\! \mathbf{x}')\, G(\mathbf{x} \!\leftrightarrow\! \mathbf{x}')}{p(\mathbf{x})}\, f_\mathrm{s}(\mathbf{x} \!\rightarrow\! \mathbf{x}' \!\rightarrow\! \mathbf{x}'')$$

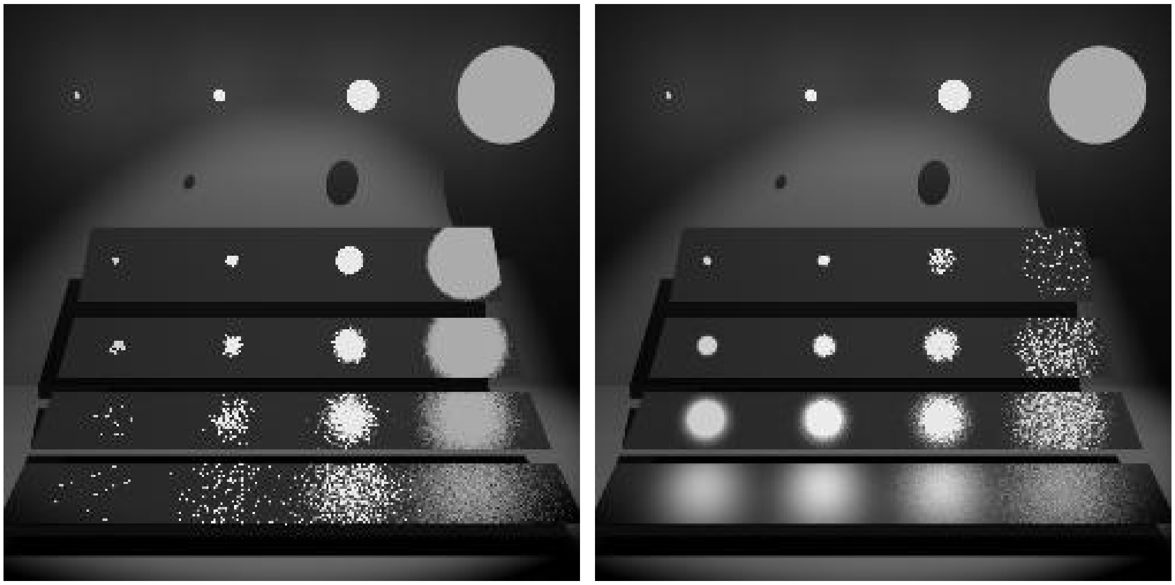

(a) Sampling the BSDF

(b) Sampling the light sources

Figure 9.2: A comparison of two sampling techniques for glossy highlights from area light sources. There are four spherical light sources of varying radii and color, plus a spotlight overhead. All spherical light sources emit the same total power. There are also four shiny rectangular plates, each one tilted so that we see the reflected light sources. The plates have varying degrees of surface roughness, which controls how sharp or fuzzy the reflections are.

Given a viewing ray that strikes a glossy surface (see Figure 9.1), images (a) and (b) use different sampling techniques for the highlight calculation. Both images are 500 by 500 pixels.

(a) Incident directions ω'_{i} are chosen with probability proportional to the BSDF $f_{\mathrm{s}}(\mathbf{x}', \omega'_{\mathrm{i}} \!\to\! \omega'_{\mathrm{o}})$, using $n_1 = 4$ samples per pixel. We call this strategy *sampling the BSDF*.

(b) Sample points $\mathbf{x}$ are randomly chosen on each light source S, using $n_2 = 4$ samples per pixel (per light source). The samples are uniformly distributed within the solid angle subtended by S at the current point $\mathbf{x}'$. We call this strategy *sampling the light source*.

The glossy BSDF used in these images is a symmetric, energy-conserving variation of the Phong model. The Phong exponent is $n = (1/r) - 1$, where r is the surface roughness parameter mentioned above, and $0 \leq r \leq 1$. The glossy surfaces also have a small diffuse component. Similar effects would occur with other glossy BSDF's.

is used. The image in Figure 9.2(b) was computed with this type of strategy, where samples were chosen according to the density

$$p(\mathbf{x}) \;\propto\; L_{\mathrm{e}}(\mathbf{x}\!\rightarrow\!\mathbf{x}')\,\frac{|\cos(\theta_{\mathrm{o}})|}{\|\mathbf{x}-\mathbf{x}'\|^2}$$

(measured with respect to surface area). With this strategy, the sample points $\mathbf{x}$ are uniformly distributed within the solid angle subtended by the light source at the current point $\mathbf{x}'$. (See Shirley et al. [1996] for further details on light source sampling strategies.)

9.1.3 Comparing the two strategies

One of these sampling strategies can have a much lower variance than the other, depending on the size of the light source and the surface roughness parameter. For example, if the light source is small and the material is relatively diffuse, then sampling the light source gives far better results than sampling the BSDF (compare the lower left portions of the images in Figure 9.2). On the other hand, if the light source is large and the material is highly polished, then sampling the BSDF is far superior (compare the upper right portions of Figure 9.2).

In both these cases, high variance is caused by inadequate sampling where the integrand is large. To understand this, notice that the integrand in the scattering equation (9.2) is a product of various factors — the BSDF f_{s}, the emitted radiance L_{e}, and several geometric quantities. The ideal density function for sampling would be proportional to the product of all of these factors, according to the principle that the variance is zero when $p(x) \propto f(x)$ (see Chapter 2).

However, neither sampling strategy takes all of these factors into account. For example, the light source sampling strategy does not consider the BSDF of the glossy surface. Thus when the BSDF has a large influence on the overall shape of the integrand (e.g. when it is a narrow, peaked function), then sampling the light source leads to high variance. On the other hand, the BSDF sampling strategy does not consider the emitted radiance function L_{e}. Thus it leads to high variance when the emission function dominates the shape of the integrand (e.g. when the light source is very small). As a consequence of these two effects, neither sampling strategy is effective over the entire range of light source geometries and surface finishes.

It is important to realize that both strategies are importance sampling techniques aimed at generating sample points on the same domain. This domain can be modeled as either a set of directions, as in equation (9.1), or a set of surface points, as in equation (9.2). For example, the BSDF sampling strategy can be expressed as a distribution over the surface of the light source, using the relationship

$$p(\mathbf{x}) \;=\; p(\omega_{\mathrm{i}}')\,\frac{d\sigma^{\perp}(\omega_{\mathrm{i}}')}{dA(\mathbf{x})} \;=\; p(\omega_{\mathrm{i}}')\,\frac{|\cos(\theta_{\mathrm{o}})\,\cos(\theta_{\mathrm{i}}')|}{\|\mathbf{x}-\mathbf{x}'\|^2} \tag{9.3}$$

(as discussed in Section 8.2.2.2). This formula makes it possible to convert a directional density into an area density, so that we can express the two sampling strategies as different probability distributions on the same domain.

9.1.4 Discussion

There are many problems in graphics that are similar to the glossy highlights example, where a large number of integrals of a specific form must be evaluated. The integrands generally have a known structure (e.g. $f(x) = f_1(x)f_2(x) + f_3(x)$), but they also depend on various parameters of the scene model (e.g. the surface roughness and light source geometry in the example above). This makes it difficult to design an adequate sampling strategy, since the parameter values are not known in advance. Furthermore, different integrals may have different parameter values even within the same scene (e.g. they may change from pixel to pixel).

The main issue is that we would like low-variance results for the entire range of parameter values, i.e. for all of the potential integrands that are obtained as these parameters vary. Unfortunately, it is often difficult to achieve this. The problem is that the integrand is usually a sum or product of many different factors, and is too complicated to sample from directly. Instead, samples are chosen from a density function that is proportional to some subset of the factors (e.g. the BSDF sampling strategy outlined above). This can lead to high variance when one of the unconsidered factors has a large effect on the integrand.

We propose a new strategy for this kind of integration problem, called *multiple importance sampling*. It is based on the idea of taking samples using several different techniques, designed to sample different features of the integrand. For example, suppose that the integrand has the form

$$f \;=\; (f_1 + f_2)\, f_3\,.$$

If the functions f_i are simple enough to be sampled directly, then the density functions $p_i \propto f_i$ would all be good candidates for sampling. Similarly, if the integrand is a product

$$f \;=\; f_1\, f_2\, \cdots\, f_k\,,$$

then several different density functions p_i could be chosen, each proportional to the product of a different set of f_i. In this way, it is often possible to find a set of importance sampling techniques that cover the various factors that can cause high variance.

Our main concern in this chapter is not how to construct a suitable set of sampling techniques, or even how to determine the number of samples that should be taken from each one. Instead, we consider the problem of how these samples should be combined, once they have been taken. We will show how to do this in a way that is unbiased, and with a variance is provably close to optimal.

In the glossy highlights problem, for example, we propose taking samples using both the BSDF and light source sampling strategies. We then show how these samples can be automatically combined to obtain low-variance results over the entire range of surface roughness and light source parameters. (For a preview of our results on this test case, see Figure 9.8.)

9.2 Multiple importance sampling

In this section, we show how Monte Carlo integration can be made more robust by using more than one sampling technique to evaluate the same integral. Our main results are on how to combine the samples: we propose strategies that are provably good compared to any other unbiased method. This makes it possible to construct estimators that have low variance for a broad class of integrands.

We start by describing a general model for combining samples from multiple techniques, called the *multi-sample model*. Using this model, any unbiased method of combining the samples can be represented as a set of weighting functions. This gives us a large space of possible combination strategies to explore, and a uniform way to represent them.

We then present a provably good strategy for combining the samples, which we call the *balance heuristic*. We show that this method gives a variance that is smaller than any other unbiased combination strategy, to within a small additive term. The method is simple and practical, and can make Monte Carlo calculations significantly more robust. We also propose several other combination strategies, which are basically refinements of the balance heuristic: they retain its provably good behavior in general, but are designed to have lower variance in a common special case. For this reason, they are often preferable to the balance heuristic in practice.

We conclude by considering a different model for how the samples are taken and combined, called the *one-sample model*. Under this model, the integral is estimated by choosing one of the n sampling techniques at random, and then taking a single sample from it. Again we consider how to minimize variance by weighting the samples, and we show that for this model the balance heuristic is optimal.

9.2.1 The multi-sample model

In order to prove anything about our methods, there must be a precise model for how the samples are taken and combined. For most of this chapter, we will use the *multi-sample model* described below. This model allows any unbiased combination strategy to be encoded as a set of weighting functions.

We consider the evaluation of an integral

$$\int_{\Omega} f(x)\, d\mu(x)\,,$$

where the domain Ω, the function $f : \Omega \to \mathbb{R}$, and the measure μ are all given. We are also given a set of n different sampling techniques on the domain Ω, whose corresponding density functions are labeled $p_1, \ldots, p_n$. We assume that only the following operations are available:

- Given any point $x \in \Omega$, $f(x)$ and $p_i(x)$ can be evaluated.

- It is possible to generate a sample X distributed according to any of the p_i.

To estimate the integral, several samples are generated using each of the given techniques. We let n_i denote the number of samples from p_i, where $n_i \geq 1$, and we let $N = \sum n_i$ denote the total number of samples. We assume that the number of samples from each technique is fixed in advance, before any samples are taken. (We do not consider the problem of how to allocate samples among the techniques; this is an interesting problem in itself, which will be discussed further in Section 9.4.2.) The samples from technique i are denoted $X_{i,j}$, for $j = 1, \ldots, n_i$. All samples are assumed to be independent, i.e. new random bits are generated to control the selection of each one.

9.2.1.1 The multi-sample estimator

We now examine how the samples $X_{i,j}$ can be used to estimate the desired integral. Our goal is generality: given any unbiased way of combining the samples, there should be a way to represent it. To do this, we consider estimators that allow the samples to be weighted differently, depending on which technique p_i they were sampled from. Each estimator has an associated set of weighting functions $w_1, \ldots, w_n$ which give the weight $w_i(x)$ for each sample x drawn from p_i. The *multi-sample estimator* is then given by

$$F \;=\; \sum_{i=1}^{n} \frac{1}{n_i} \sum_{j=1}^{n_i} w_i(X_{i,j}) \, \frac{f(X_{i,j})}{p_i(X_{i,j})} \,. \tag{9.4}$$

This formula can be thought of as a weighted sum of the estimators $f(X_{i,j})/p_i(X_{i,j})$ that would be obtained by using each sampling technique p_i on its own. Notice that the weights are not constant, but can vary as a function of the sample point $X_{i,j}$.

For this estimate to be unbiased, the weighting functions w_i must satisfy the following two conditions:

(W1) $\sum_{i=1}^{n} w_i(x) \;=\; 1$ whenever $f(x) \neq 0$, and

(W2) $w_i(x) = 0$ whenever $p_i(x) = 0$.

These conditions imply the following corollary: at any point where $f(x) \neq 0$, at least one of the $p_i(x)$ must be positive (i.e., at least one sampling technique must be able to generate samples there). Thus on the other hand, it is not necessary for every p_i to sample the whole domain; it is allowable for some of the p_i to be specialized sampling techniques that concentrate on specific regions of the integrand.[1]

Given that (W1) and (W2) hold, the following lemma states that F is unbiased:

Lemma 9.1. *Let F be any estimator of the form (9.4), where $n_i \geq 1$ for all i, and the weighting functions w_i satisfy conditions (W1) and (W2). Then*

$$E[F] \;=\; \int_\Omega f(x)\, d\mu(x)\,.$$

Proof.

$$\begin{aligned} E[F] \;&=\; \sum_{i=1}^{n} \frac{1}{n_i} \sum_{j=1}^{n_i} \int_\Omega \frac{w_i(x)\, f(x)}{p_i(x)}\, p_i(x)\, d\mu(x) \\ &=\; \int_\Omega \sum_{i=1}^{n} w_i(x)\, f(x)\, d\mu(x) \\ &=\; \int_\Omega f(x)\, d\mu(x)\,. \quad \blacksquare \end{aligned}$$

The remainder of this section is devoted to showing the generality of the multi-sample model. We show that by choosing the weighting functions appropriately, it is possible to represent virtually any unbiased combination strategy. To make this more concrete, we first give some examples of possible strategies, and show how to represent them by weighting functions. We then show how the multi-sample estimator can be rewritten in a different form that makes its generality more obvious. This leads up to Section 9.2.2, where we will describe a new combination strategy that has provably good performance compared to all strategies that the multi-sample model can represent.

9.2.1.2 Examples of weighting functions

Suppose that there are three sampling techniques p_1, p_2, and p_3, and that a single sample $X_{i,1}$ is taken from each one ($n_1 = n_2 = n_3 = 1$). First, consider the case where the weighting

[1] If f is allowed to contain Dirac distributions, note that (W2) should be modified to state that $w_i(x) = 0$ whenever $f(x)/p_i(x)$ is not finite. To relate this to graphics, consider a mirror which also reflects some light diffusely. The modified (W2) states that samples from the diffuse component cannot be used to estimate the specular contribution, since this corresponds to the situation where $f(x)$ contains a Dirac distribution $\delta(\mathbf{x} - \mathbf{x}_0)$, but $p(x)$ does not.)

functions are constant over the whole domain Ω. This leads to the estimator

$$F \;=\; w_1 \frac{f(X_{1,1})}{p_1(X_{1,1})} + w_2 \frac{f(X_{2,1})}{p_2(X_{2,1})} + w_3 \frac{f(X_{3,1})}{p_3(X_{3,1})}\,,$$

where the w_i sum to one. This estimator is simply a weighted combination of the estimators $F_i \;=\; f(X_{i,1}) \,/\, p_i(X_{i,1})$ that would be obtained by using each of the sampling techniques alone. Unfortunately, this combination strategy does not work very well: if any of the given sampling techniques is bad (i.e. the corresponding estimator F_i has high variance), then F will have high variance as well, since

$$V[F] \;=\; w_1 V[F_1] + w_2 V[F_2] + w_3 V[F_3]\,.$$

Another possible combination strategy is to partition the domain among the sampling techniques. To do this, the integral is written in the form

$$\int_\Omega f(x)\, d\mu(x) \;=\; \sum_{i=1}^{n} \int_{\Omega_i} f(x)\, d\mu(x)\,,$$

where the Ω_i are non-overlapping regions whose union is Ω. The integral is then estimated in each region Ω_i separately, using samples from just one technique p_i. In terms of weighting functions, this is represented by letting

$$w_i(x) \;=\; \begin{cases} 1 & \text{if } x \in \Omega_i\,, \\ 0 & \text{otherwise}\,. \end{cases}$$

This combination strategy is used a great deal in computer graphics; however, sometimes it does not work very well due to the simple partitioning rules that are used. For example, it is common to evaluate the scattering equation by dividing the scene into light source regions and non-light-source regions, which are sampled using different techniques (e.g. sampling L_{e} vs. sampling the BSDF). Depending on the geometry and materials of the scene, this fixed partitioning can lead to a much higher variance than necessary (as we saw in the glossy highlights example).

Another combination technique that is often used in graphics is to write the integrand as a sum $f = \sum g_i$, and use a different sampling technique to estimate the contribution of each g_i. For example, this occurs when the BSDF is split into diffuse, glossy, and specular components, whose contributions are estimated separately (by sampling from density functions $p_i \propto g_i$). As before, it is straightforward to represent this strategy as a set of weighting functions.

9.2.1.3 Generality of the multi-sample model

The generality of this model can be seen more easily by rewriting the multi-sample estimator (9.4) in the form

$$F \;=\; \sum_{i=1}^{n} \sum_{j=1}^{n_i} C_i(X_{i,j})\,, \tag{9.5}$$

where $C_i(X_{i,j})$ is the called the *sample contribution* for $X_{i,j}$. The functions C_i are arbitrary, except that in order for F to be unbiased they must satisfy

$$\sum_{i=1}^{n} n_i\, C_i(x)\, p_i(x) \;=\; f(x) \tag{9.6}$$

at each point $x \in \Omega$. In this form, it is clear that the multi-sample model can represent any unbiased combination strategy, subject only to the assumptions that all samples are taken independently, and that our knowledge of f and p_i is limited to point evaluation. (This forces the estimator to be unbiased at each point x independently, as expressed by condition (9.6).)

To see that this formulation of the multi-sample model is equivalent to the original one, we simply let

$$C_i(x) \;=\; \frac{w_i(x)\, f(x)}{n_i\, p_i(x)}\,. \tag{9.7}$$

It is easy to verify that if the weighting functions w_i satisfy conditions (W1) and (W2), then the corresponding contributions C_i satisfy (9.6), and vice versa. The main reason for preferring the w_i formulation is that the corresponding conditions are easier to satisfy.

9.2.2 The balance heuristic

The multi-sample model gives us a large space of unbiased estimators to explore, and a uniform way to represent them (as a set of weighting functions). Our goal is now to find the estimator F with minimum variance, by choosing the w_i appropriately.

We will show that the following weighting functions are a good choice:

$$\hat{w}_i(x) \;=\; \frac{n_i\, p_i(x)}{\sum_k \, n_k\, p_k(x)}\,. \tag{9.8}$$

We call this strategy the *balance heuristic*.[2] The key feature of the balance heuristic is that no other combination strategy is much better, as stated by the following theorem:

Theorem 9.2. *Let f, n_i, and p_i be given, for $i = 1, \ldots, n$. Let F be any unbiased estimator of the form (9.4), and let $\hat{F}$ be the estimator that uses the weighting functions $\hat{w}_i$ (the balance heuristic). Then*

$$V[\hat{F}] - V[F] \;\leq\; \left(\frac{1}{\min_i n_i} - \frac{1}{\sum_i n_i} \right) \mu^2\,, \tag{9.9}$$

where $\mu = E[F] = E[\hat{F}]$ is the quantity to be estimated. (A proof is given in Appendix 9.A.)

According to this result, no other combination strategy can significantly improve upon the balance heuristic. That is, suppose that we let F^* denote the *best possible* combination strategy for a particular problem (i.e. for a given choice of the f, p_i, and n_i). In general, we have no way of knowing what this strategy is: for example, suppose that one of the p_i is exactly proportional to f, so that the best strategy is to ignore any samples taken with the other techniques, and use only the samples from p_i. We cannot hope to discover this fact from a practical point of view, since our knowledge of f and p_i is limited to point sampling and evaluation. Nevertheless, even compared to this unknown optimal strategy F^*, the balance heuristic is almost as good: its variance is worse by at most the term on the right-hand side of (9.9).

To give some intuition about this upper bound on the "variance gap", suppose that there are just two sampling techniques, and that $n_1 = n_2 = 4$ samples are taken from each one. In this case, the variance of the balance heuristic is optimal to within an additive term of $\mu^2/8$. In familiar graphics terms, this corresponds to the variance obtained by sending 8 shadow

[2] The name refers to the fact that the sample contributions are "balanced" so that they are the same for all techniques i:

$$C_i(x) \;=\; \frac{\hat{w}_i(x)\, f(x)}{n_i\, p_i(x)} \;=\; \frac{f(x)}{\sum_k \, n_k\, p_k(x)}\,.$$

That is, the contribution $C_i(X_{i,j})$ of a sample $X_{i,j}$ does not depend on which technique i generated it.

rays to an area light source that is 50% occluded. Furthermore, notice that the variance gap goes to zero as the number of samples from each technique is increased. On the other hand, if a poor combination strategy is used then the variance can be larger than optimal by an arbitrary amount. This is essentially what we observed in the glossy highlights images of Figure 9.2: if the wrong samples are used to estimate the integral, the variance can be tens or hundreds of times larger than μ^2.

Furthermore, the balance heuristic is practical to implement. The main requirement for evaluating the weighting functions $\hat{w}_i$ is that given any point x, we must be able to evaluate the probability densities $p_k(x)$ for all k. This situation is different than for the usual estimator $f(X)/p(X)$, where it is only necessary to evaluate $p(X)$ for sample points generated using p. The balance heuristic requires slightly more than this: given a sample $X_{i,j}$ generated using technique p_i, we also need to evaluate the probabilities $p_k(X_{i,j})$ with which all of the *other* $n-1$ techniques generate that sample point. It is usually straightforward to do this; it is just a matter of reorganizing the routines that compute probabilities, and expressing all densities with respect to the same measure.

For example, consider the glossy highlights problem of Section 9.1. To evaluate the weighting function $\hat{w}_i$ for each sample point x, we compute the probability density for generating x using both sampling techniques. Thus if x was generated by sampling the light source, then we also compute the probability density for generating the same point x by sampling the BSDF (as discussed in Section 9.1.3). Note that the cost of computing these extra probabilities is insignificant compared to the other calculations involved, such as ray casting; details will be given in Section 9.3.

9.2.2.1 A simple interpretation of the balance heuristic

By writing the balance heuristic in a different form, we will show that it is actually a very natural way to combine samples from multiple techniques.

To do this, we insert the weighting functions $\hat{w}_i$ into the multi-sample estimator (9.4), yielding

$$\hat{F} \;=\; \sum_{i=1}^{n} \frac{1}{n_i} \sum_{j=1}^{n_i} \left(\frac{n_i\, p_i(X_{i,j})}{\sum_k \, n_k\, p_k(X_{i,j})} \right) \frac{f(X_{i,j})}{p_i(X_{i,j})}$$

$$
\begin{aligned}
&= \sum_{i=1}^{n} \sum_{j=1}^{n_i} \frac{f(X_{i,j})}{\sum_k \, n_k \, p_k(X_{i,j})} \\
&= \frac{1}{N} \sum_{i=1}^{n} \sum_{j=1}^{n_i} \frac{f(X_{i,j})}{\sum_k \, c_k \, p_k(X_{i,j})} \,, \qquad (9.10)
\end{aligned}
$$

where $N = \sum_i n_i$ is the total number of samples, and $c_k = n_k / N$ is the fraction of samples from p_k.

In this form, the balance heuristic corresponds to a standard Monte Carlo estimator of the form f/p. This can be seen more easily by rewriting the denominator of (9.10) as

$$
\hat{p}(x) \;=\; \sum_{k=1}^{n} c_k \, p_k(x) \,, \qquad (9.11)
$$

which we call the *combined sample density*. The quantity $\hat{p}(x)$ represents the probability density for sampling the given point x, averaged over the entire sequence of N samples.[3]

Thus, the balance heuristic is natural way to combine the samples. It has the form of a standard Monte Carlo estimator, where the denominator $\hat{p}$ represents the average distribution of the whole group of samples to which it is applied. Pseudocode for this estimator is given in Figure 9.3. However, it is important to realize that the main advantage of this estimator is not that it is simple or standard, but that it has provably good performance compared to other combination strategies. This is the reason that we introduced the more complex formulation in terms of weighting functions, so that we could compare it against a family of other techniques.

9.2.3 Improved combination strategies

Although the balance heuristic is a good combination strategy, there is still some room for improvement (within the bounds given by Theorem 9.2). In this section, we discuss two families of estimators that have lower variance than the balance heuristic in a common special case. These estimators are unbiased, and like the balance heuristic, they are provably good compared to all other combination strategies.

[3] More precisely, it is the density of a random variable X that is equal to each $X_{i,j}$ with probability $1/N$.

```
function Balance-Heuristic()
    $N \leftarrow \sum_{i=1}^{n} n_i$
    for $i \leftarrow 1$ to $n$
        for $j \leftarrow 1$ to $n_i$
            $X \leftarrow$ TakeSample$(p_i)$
            $\hat{p} \leftarrow \sum_{k=1}^{n} (n_k/N)\, p_k(X)$
            $F \leftarrow F + f(X)/\hat{p}$
    return $F/N$
```

Figure 9.3: Pseudocode for the balance heuristic estimator.

We start by applying the balance heuristic to the glossy highlights problem of Section 9.1. We show that it leads to more variance than necessary in exactly those cases where the original sampling techniques did very well, e.g. where sampling the light source gave a low-variance result. The problem is that the additional variance due to the balance heuristic is additive: this is not significant when the optimal estimator already has substantial variance, but it is noticeable compared to an optimal estimator whose variance is very low.

We thus consider how to improve the performance of the balance heuristic on *low-variance problems*, i.e. those for which one of the given sampling techniques is an excellent match for the integrand. We show that the balance heuristic can be improved in this case by modifying its weighting functions slightly. In particular, we show that it is desirable to *sharpen* these weighting functions, by decreasing weights that are close to zero, and increasing weights that are close to one. We propose two general strategies for doing this, which we call the *cutoff* and *power* heuristics. The balance heuristic can be obtained as a limiting case of both these families of estimators.

Finally, we give some theoretical results showing that these new combination strategies are provably close to optimal. Thus, they are never much worse than the balance heuristic, but for low-variance problems they can be noticeably better. Later in this chapter, we will describe numerical tests that verify these results (Section 9.3). Based on these experiments, we have found that one strategy in particular is a good choice in practice: namely, the power

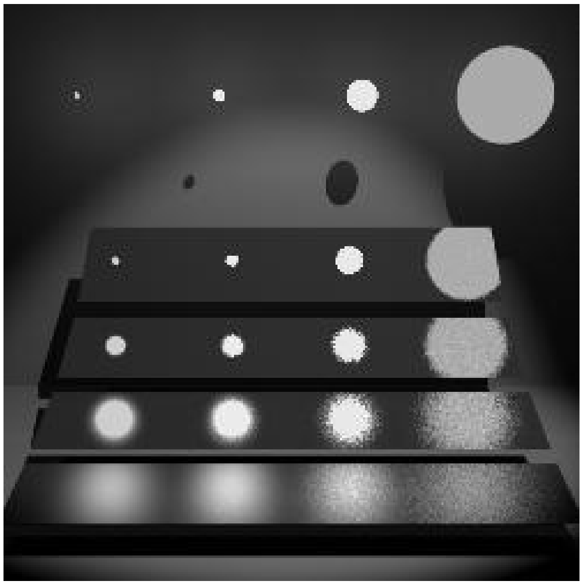

Figure 9.4: This image was rendered using both the BSDF sampling strategy and the light source sampling strategy. The samples are exactly the same as those for Figure 9.2(a) and (b), except that here the two kinds of samples are combined using the balance heuristic. This leads to a strategy that is effective over the entire range of glossy surfaces and light source geometries.

heuristic with the exponent $\beta = 2$.

9.2.3.1 Low-variance problems: examples and analysis

Figure 9.4 shows the balance heuristic applied to glossy highlights problem of Section 9.1. This image combines the samples from Figure 9.2(a) and (b), which used the BSDF and light source sampling strategies respectively. By combining both kinds of samples, we obtain a strategy that works well over the entire range of surface finishes and light source geometries.

In some regions of the image, however, the balance heuristic does not work quite as well as the best of the given sampling techniques. Figure 9.5 demonstrates this, by comparing the balance heuristic against images that use the BSDF or light source samples alone. Columns (a), (b), and (c) show close-ups of the images in Figure 9.2(a), Figure 9.2(b), and Figure 9.4 respectively. To make the differences more obvious, these images were computed using

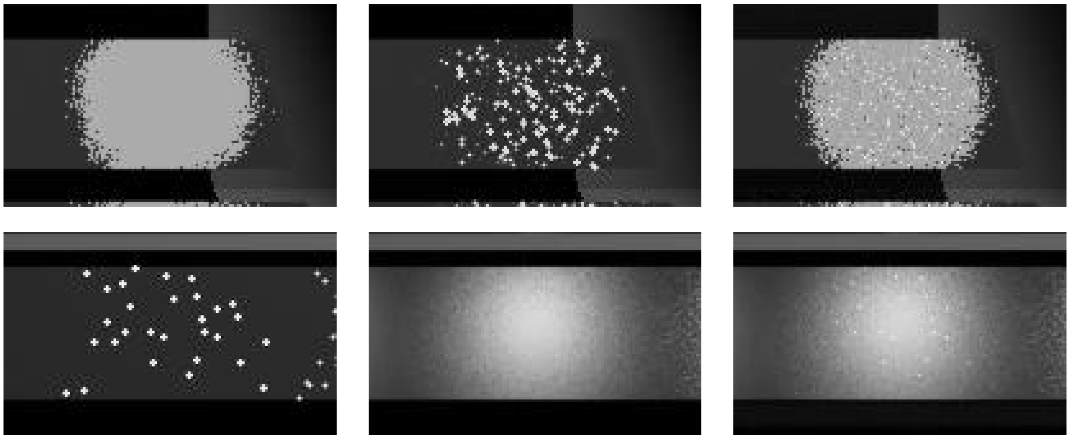

(a) Sampling the BSDF **(b)** Sampling the lights **(c)** The balance heuristic

Figure 9.5: These images show close-ups of the glossy highlights test scene, computed by **(a)** sampling the BSDF, **(b)** sampling the light sources, and **(c)** the balance heuristic. Notice that although the balance heuristic works much better than one of the two techniques in each region, it does not work quite as well as the other. These images were computed with one sample per pixel from each technique ($n_1 = n_2 = 1$), as opposed to the four samples per pixel used in Figures 9.2 and 9.4, in order to reveal the noise differences more clearly.

only one sample per pixel (as opposed to the four samples per pixel used in the source images.) It is clear that although the balance heuristic works far better in each region than the technique whose variance is high, it has some additional noise compared to the technique whose variance is low.

The test cases in Figure 9.5 are examples of *low-variance problems*, which occur when one of the given sampling techniques p_i is an extremely good match for the integrand f. In this situation it is possible to construct an estimator whose variance is nearly zero, by taking samples using p_i and applying the standard estimate f/p_i. The balance heuristic can be noticeably worse than the results obtained in this way, because Theorem 9.2 only states that the variance of the balance heuristic is optimal to within an additive extra term. Even though this extra variance is guaranteed to be small on an absolute scale, it can still be noticeable compared to an optimal variance that is practically zero (especially if only a few samples are taken).

Unfortunately, there is no way to reliably detect this situation under the point sampling

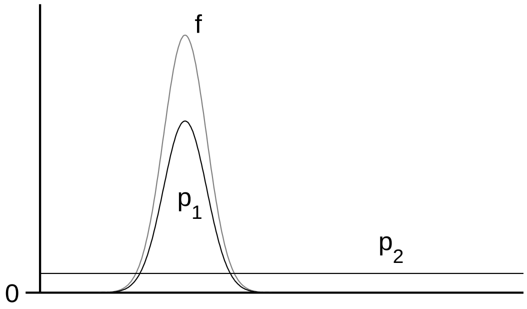

Figure 9.6: Two density functions for sampling a simple integrand.

assumptions of the multi-sample model. Instead, our strategy is to take samples using all of the given techniques, and compute weighting functions that automatically assign low weights to any irrelevant samples. In the case where one of the p_i is a good match for f, the ideal result would be to compute weighting functions such that $w_i(x) = 1$ over the whole domain, while all of the other w_j are zero. This would achieve the same end result as using p_i alone, at the expense of taking several unnecessary samples from the other p_j. However, extra sampling is unavoidable if we do not know in advance which of the given sampling techniques will work best.

We now consider how the balance heuristic can be improved, so that it performs better on low-variance problems. To do this, we study the simple test case of Figure 9.6, which shows an integrand f and two density functions p_1 and p_2 to be used for importance sampling. The density function p_1 is proportional to f, while p_2 is a constant function. For this situation, the optimal weighting functions are obviously

$$\begin{aligned} w_1^*(x) &\equiv 1\,, \\ w_2^*(x) &\equiv 0\,, \end{aligned}$$

since this would give an estimator F^* whose variance is zero.

The balance heuristic weighting functions $\hat{w}_i$ are different than the optimal ones above, and thus the balance heuristic will lead to additional variance. We now examine where this extra variance comes from, to see how it can be reduced. We start by dividing the domain

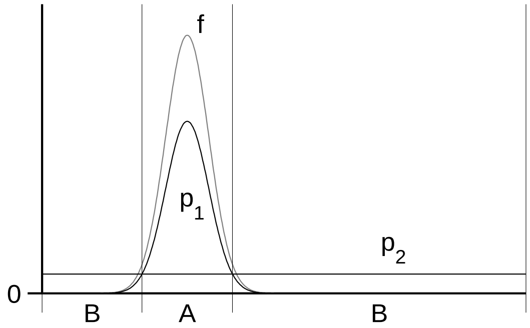

Figure 9.7: The integration domain is divided into two regions A and B. Region A represents the set of points where $p_1 > p_2$, while region B represents the points where $p_2 > p_1$. The weights computed by the balance heuristic are considered in each region separately.

into two regions A and B, as shown in Figure 9.7. Region A represents the set of points where $p_1 > p_2$, while region B represents the points where $p_2 > p_1$. We will consider the weights computed by the balance heuristic in each region separately. To simplify the discussion, we assume that $n_1 = n_2 = 1$ (i.e. a single sample is taken using each technique, and their contributions are summed).

First consider the sample from p_1, which is likely to occur in the central part of region A. Since p_1 is much larger than p_2 in this region, the sample weight $\hat{w}_1 = p_1/(p_1 + p_2)$ will be close to one. This agrees with the optimal weighting function $w_1^* = 1$, as desired.

Similarly, the sample from p_2 is likely to occur in region B, where its weight $\hat{w}_2 = p_2/(p_1 + p_2)$ is close to one. Nevertheless, the contribution of this sample will be small, since the integrand f is nearly zero in region B. Therefore this situation is also close to the optimal one, in which the samples from p_2 are ignored.

However, there are two effects that lead to additional variance. First, the sample from p_1 sometimes occurs near the boundaries of region A (or even in region B), where its weight $\hat{w}_1 = p_1/(p_1 + p_2)$ is significantly smaller than one. In this case, the sample makes a contribution that is noticeably smaller than the optimal value f/p_1. (Recall that p_1 is proportional to f, so that f/p_1 is the desired value μ of the integral.) In Figure 9.5, this effect shows up as occasional pixels that are darker than they should be (e.g. in the top image of column (c)).

The second problem is that the sample from p_2 sometimes occurs in region A. When this happens, its weight $\hat{w}_2 = p_2/(p_1 + p_2)$ is small. However, the contribution made by this sample is

$$\hat{w}_2 \, \frac{f}{p_2} \;=\; \frac{p_2}{p_1 + p_2} \, \frac{f}{p_2} \;=\; \frac{f}{p_1 + p_2}\,,$$

which is approximately equal to $f/p_1 = \mu$ in this region. Since it is likely that the sample from p_1 also lies in region A (contributing another μ toward the estimate), this leads to a total estimate of approximately 2μ. In Figure 9.5(c), this effect shows up as occasional pixels that are approximately twice as bright as their neighbors.[4]

Thus, the additional noise of the balance heuristic can be attributed to two problems. First, some of the samples from p_1 have weights that are significantly smaller than one: this happens near the boundary of region A, where p_1 and p_2 have comparable magnitude. (Very few of these samples will occur in the region where $p_1 \ll p_2$, simply because p_1 is very small there.) The second problem is that some samples from p_2 make contributions of noticeable size (i.e. a significant fraction of μ). Most of these samples have small weights, because they occur in region A where $p_1 > p_2$. Some samples will also occur in the region where p_1 and p_2 have comparable magnitude; however, the samples where $p_2 \gg p_1$ do not cause any problems, since the sample contribution $f/(p_1 + p_2)$ is negligible there.

9.2.3.2 Better strategies for low-variance problems

We now present two families of combination strategies that have better performance on low-variance problems. These strategies are variations of the balance heuristic, where the weighting functions have been *sharpened* by making large weights closer to one and small weights closer to zero. This idea is effective at reducing both sources of variance described above.

The basic observation is that most samples from p_1 occur in region A, where $p_1 > p_2$. We would like all of these samples to have the optimal weight $w_1^* = 1$. Since the balance heuristic already assigns these samples a weight $\hat{w}_1 = p_1/(p_1 + p_2)$ that is greater than $1/2$, we can get closer to the optimal weighting functions by applying the sharpening strategy mentioned above. For example, one way to do this would be to set $w_1 = 1$ (and $w_2 = 0$)

[4] Note that this situation is entirely different than the "spikes" of Figure 9.5(a) and (b), which are caused by sample contributions that are hundreds of times larger than the desired mean value.

whenever $\hat{w}_1 > 1/2$.

Similarly, this idea can reduce the variance caused by samples from p_2 in region A. The optimal weight for these samples is $w_2^* = 0$, while the balance heuristic assigns them a weight $\hat{w}_2 < 1/2$, so that sharpening the weighting functions is once again an effective strategy.[5]

We now describe two different combination strategies that implement this sharpening idea, called the *cutoff heuristic* and the *power heuristic*. Each of these is actually a family of strategies, controlled by an additional parameter. For convenience in describing them, we will drop the x argument on the functions w_i and p_i, and define a new symbol q_i as the product $q_i = n_i p_i$. For example, in this notation the balance heuristic would be written as

$$\hat{w}_i = \frac{q_i}{\sum_k q_k} .$$

The cutoff heuristic. The *cutoff heuristic* modifies the weighting functions by discarding samples with low weight, according to a cutoff threshold $\alpha \in [0, 1]$:

$$w_i = \begin{cases} 0 & \text{if } q_i < \alpha\, q_{\max} \\ \dfrac{q_i}{\sum_k \{q_k \mid q_k \geq \alpha\, q_{\max}\}} & \text{otherwise} \end{cases} \tag{9.12}$$

where $q_{\max} = \max_k q_k$. The threshold α determines how small q_i must be (compared to $q_{\max}$) before it is thrown away.

The power heuristic. The *power heuristic* modifies the weighting functions in a different way, by raising all of the weights to an exponent β, and then renormalizing:

$$w_i = \frac{q_i^\beta}{\sum_k q_k^\beta} . \tag{9.13}$$

[5] Note that sharpening the weighting functions is not a perfect solution for low-variance problems, since it does not address the extra variance due to samples in region B (where $p_2 > p_1$). In this region, sharpening the weighting functions has the effect of decreasing w_1 and increasing w_2, which is opposite to what is desired. The number of samples affected in this way is relatively small, however, under the assumption that most samples from p_1 occur where $p_1 \gg p_2$.

We have found the exponent $\beta = 2$ to be a reasonable value. With this choice, the sample contribution $(w_i\, f)/(n_i\, p_i)$ is proportional to p_i, so that it decreases gradually as p_i becomes smaller relative to the other p_k. (Compare this with the balance heuristic, where a sample at a given point x always makes the same contribution, no matter which sampling technique generated it.)

Notice that the balance heuristic can be obtained as a limiting case of both strategies (when $\alpha = 0$ or $\beta = 1$). These two strategies also share another limiting case, obtained by setting $\alpha = 1$ or $\beta = \infty$. This special case is called the *maximum heuristic*:

The maximum heuristic. The maximum heuristic partitions the domain into n regions, according to which function q_i is largest at each point x:

$$w_i \;=\; \begin{cases} 1 & \text{if } q_i = q_{\max} \\ 0 & \text{otherwise}\,. \end{cases} \tag{9.14}$$

In other words, samples from p_i are used to estimate the integral only in the region Ω_i where $w_i = 1$. The maximum heuristic does not work as well as the other strategies in practice; intuitively, this is because too many samples are thrown away. However, it gives some insight into the other combination strategies, and has an elegant structure.

9.2.3.3 Variance bounds

The advantage of these strategies is reduced variance when one of the p_i is a good match for f. Their performance is otherwise similar to the balance heuristic; it is possible to show they are never much worse. In particular, we have the following worst-case bounds:

Theorem 9.3. *Let f, n_i, and p_i be given, for $i = 1, \ldots, n$. Let F be any unbiased estimator of the form (9.4), and let F' be one of the estimators described above. Then the variance of F' satisfies a bound of the form*

$$V[F'] \;\le\; c\, V[F] + \left(\frac{1}{\min_i n_i} - \frac{1}{\sum_i n_i}\right) \mu^2\,,$$

where the constant c is given by the following table:

Cutoff heuristic (with threshold α)	$c \;=\; 1 + \alpha\,(n-1)$
Power heuristic (with exponent β)	$c = 1 + (1/\beta)^{1/\beta}\,((n-1)(1-1/\beta))^{1-1/\beta}$
Power heuristic (with exponent $\beta = 2$)	$c \;=\; (1/2)\,(1+\sqrt{n})$

In particular, these bounds hold when F' is compared against the unknown, optimal estimator F^*. A proof of this theorem in given in Appendix 9.A. However, the true test of these strategies is how they perform on practical problems; measurements along these lines are presented in Section 9.3.1.

9.2.4 The one-sample model

We conclude by considering a different model for how the samples are taken and combined, called the *one-sample model*. Under this model, the integral is estimated by choosing one of the n sampling techniques at random, and then taking a single sample from it. Again we consider how to minimize variance by weighting the samples, and we show that for this model the balance heuristic is optimal: no other combination technique has smaller variance.

Let p_1, …, p_n be the density functions for the n given sampling techniques. To generate a sample, one of the density functions p_i is chosen at random according to a given set of probabilities c_1, …, c_n (which sum to one). A single sample is then taken from the chosen technique. This sampling model is often used in graphics: for example, it describes algorithms such as path tracing, where sampling the BSDF may require a random choice between different techniques for the diffuse, glossy, and specular components.

As before, we consider a family of unbiased estimators for the given integral $\int_\Omega f(x)\,d\mu(x)$, where each estimator is represented by a set of weighting functions w_1, …, w_n. The process of choosing a sampling technique, taking a sample, and computing a weighted estimate is then expressed by the *one-sample estimator*

$$F \;=\; \frac{w_I(X_I)\,f(X_I)}{c_I\,p_I(X_I)}\,, \tag{9.15}$$

where $I \in \{1,\ldots,n\}$ is a random variable distributed according to the probabilities c_i, and

X_I is a sample from the corresponding technique p_I. This estimator is unbiased under the same conditions on the w_i discussed in Section 9.2.1.

We now consider how to choose the weighting functions w_i, to minimize the variance of the resulting estimator. We can show that for this model, the balance heuristic is optimal:

Theorem 9.4. *Let f, c_i, and p_i be given, for $i = 1, \ldots, n$. Let F be any unbiased estimator of the form (9.15), and let $\hat{F}$ be the corresponding estimator that uses the balance heuristic weighting functions (9.8). Then*

$$V[\hat{F}] \;\leq\; V[F]\,.$$

(A proof is given in Appendix 9.A.) Thus, for this sampling model the improved combination strategies of Section 9.2.3 are unnecessary.

9.3 Results

In this section, we show how multiple importance sampling can be applied to two important application areas: distribution ray tracing (in particular, the glossy highlights problem from Section 9.1), and the *final gather* pass of certain light transport algorithms. (In the next chapter we will describe a more advanced example of our techniques, namely bidirectional path tracing.)

9.3.1 The glossy highlights problem

Our first test is the computation of glossy highlights from area light sources (previously described in Section 9.1). As can be seen in Figure 9.8(a) and (b), sampling the BSDF works well for sharp reflections of large light sources, while sampling the light source works well for fuzzy reflections of small light sources. In Figure 9.8(c), we have used the power heuristic with $\beta = 2$ to combine both kinds of samples. This method works very well for all light source/BSDF combinations. Figure 9.8(d) is a visualization of the weighting functions that were used to compute this image.

To compare the various combination strategies (the balance, cutoff, power, and maximum heuristics), we have measured the variance numerically as a function of the surface

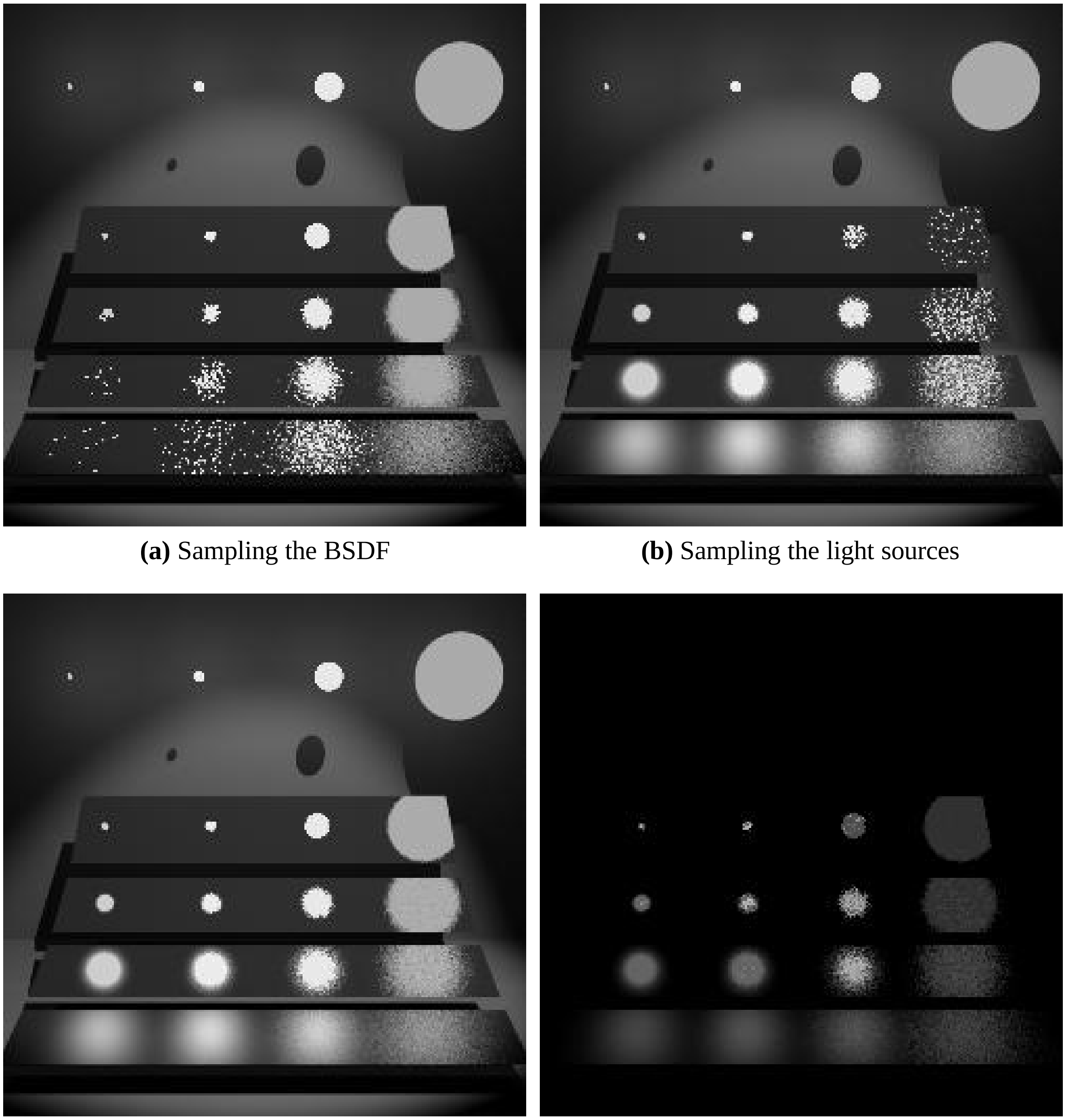

(a) Sampling the BSDF

(b) Sampling the light sources

(c) The power heuristic with $\beta = 2$.

(d) The weights used by the power heuristic.

Figure 9.8: Multiple importance sampling applied to the glossy highlights problem. **(a)** and **(b)** are the images from Figure 9.2, computed by sampling the BSDF and sampling the light sources respectively. **(c)** was computed by combining the samples from (a) and (b) using the power heuristic with $\beta = 2$. Finally, **(d)** is a false-color image showing the weights used to compute (c). Red represents sampling of the BSDF, while green represents sampling of the light sources. Yellow indicates that both types of samples are assigned a significant weight.

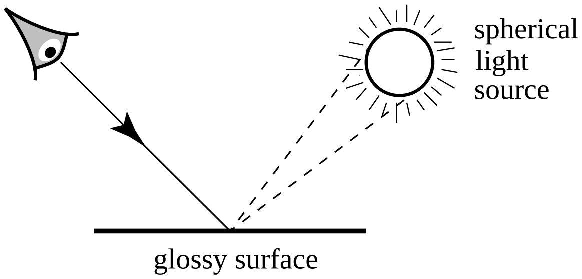

Figure 9.9: A scale diagram of the scene model used to measure the variance of the glossy highlights calculation. The glossy surface is illuminated by a single spherical light source, so that a blurred reflection of the light source is visible from the camera position. Variance was measured by taking 100,000 samples along the viewing ray shown, which intersects the center of the blurred reflection at an angle of 45 degrees. This calculation was repeated for approximately 100 different values of the surface roughness parameter r (which controls how sharp or fuzzy the reflections are), in order to measure the variance as a function of surface roughness. The light source occupies a solid angle of 0.063 radians.

roughness parameter r. Figure 9.9 shows the test setup, and the results are summarized in Figure 9.10. Three curves are shown in each graph: two of them correspond to the BSDF and light source sampling techniques, while the third corresponds to the combination strategy being tested (i.e. the balance, cutoff, power, or maximum heuristic). Each graph plots the relative error σ/μ as a function of r, where σ is the standard deviation of a single sample, and μ is the mean.

Notice that all four combination strategies yield a variance that is close to the minimum of the two other curves (on an absolute scale). This is in accordance with Theorem 9.2, which guarantees that the variance σ^2 of the balance heuristic is within $\mu^2/2$ of the variance obtained when either of the given sampling techniques is used on its own. The plots in Figure 9.10(a) are well within this bound.

At the extremes of the roughness axis there are significant differences among the various combination strategies. As expected, the balance heuristic (a) performs worst at the extremes, since the other strategies were specifically designed to have better performance in this case (i.e. the case when one of the given sampling techniques is an excellent match for the integrand). The power heuristic (c) with $\beta = 2$ works especially well over the entire range of roughness values.

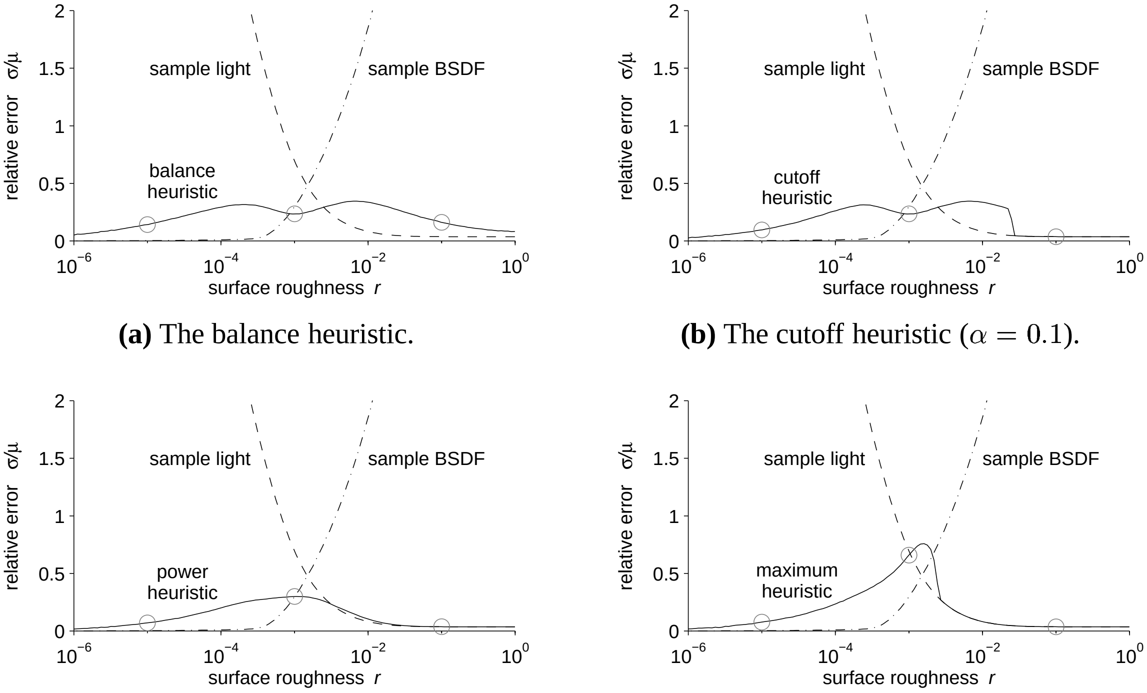

(a) The balance heuristic.

(b) The cutoff heuristic ($\alpha = 0.1$).

(c) The power heuristic ($\beta = 2$).

(d) The maximum heuristic.

Figure 9.10: Variance measurements for the glossy highlights problem using different combination strategies. Each graph plots the relative error σ/μ as a function of the surface roughness parameter r (where σ^2 represents the variance of a single sample, and μ is the mean). A fixed size, spherical light source was used (as shown in Figure 9.9). The three curves in each graph correspond to sampling the BSDF, sampling the light source, and a weighted combination of both sample types using the (a) balance, (b) cutoff, (c) power, and (d) maximum heuristics. (The three small circles on each graph are explained in Figure 9.11.)

Figure 9.11 shows how these numerical measurements translate into actual image noise. Each image shows a glossy reflection of a spherical light source, using the same test setup as for the graphs (see Figure 9.9). The three images in each group were computed using different parameter values (namely $r = 10^{-5}$, $r = 10^{-3}$, and $r = 10^{-1}$), which causes the reflected light source to be blurred by varying amounts. The noise levels in these images should be compared against the corresponding circled variance measurements in the graphs of Figure 9.10. Notice that the cutoff, power, and maximum heuristics substantially reduce the noise at the extremes of the roughness axis.

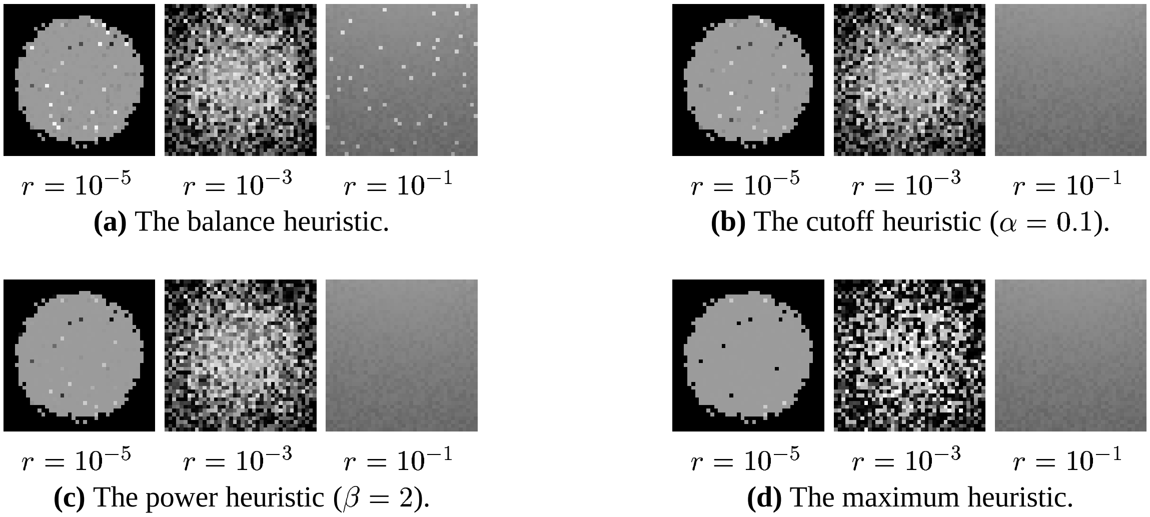

$r = 10^{-5}$ $r = 10^{-3}$ $r = 10^{-1}$

(a) The balance heuristic.

$r = 10^{-5}$ $r = 10^{-3}$ $r = 10^{-1}$

(b) The cutoff heuristic ($\alpha = 0.1$).

$r = 10^{-5}$ $r = 10^{-3}$ $r = 10^{-1}$

(c) The power heuristic ($\beta = 2$).

$r = 10^{-5}$ $r = 10^{-3}$ $r = 10^{-1}$

(d) The maximum heuristic.

Figure 9.11: Each of these test images corresponds to one of the circled points on the variance curves of Figure 9.10. Their purpose is to compare the different combination strategies visually, by showing how the numerical variance measurements translate into actual image noise. Each image shows a glossy reflection of a spherical light source, as shown in Figure 9.9 (the same test setup used for the graphs). The three images in each group were computed using different values of the surface roughness parameter r (with one sample per pixel, box filtered), which causes the reflected light source to be blurred by varying amounts (the sharpest reflections are on the left). The noise levels in these images should be compared against the corresponding circled variance measurements shown in Figure 9.10. Notice in particular that the improved weighting strategies (b), (c), and (d) give much better results when $r = 10^{-1}$, and significantly better results when $r = 10^{-5}$.

In all cases, the additional cost of multiple importance sampling was small. The total time spent evaluating probabilities and weighting functions in these tests was less than 5%. For scenes of realistic complexity, the overhead would be even smaller (as a fraction of the total computation time).

We have also made measurements of the cutoff and power heuristics using other values of α and β (which represent the cutoff threshold and the exponent, respectively). In fact, the graphs in Figure 9.10 already give results for three values of α and β each, since the balance and maximum heuristics are limiting cases of the other two strategies. Specifically, the cutoff heuristic for $\alpha = 0$, $\alpha = 0.1$, and $\alpha = 1$ is represented by graphs (a), (b), and (d), while the power heuristic for $\beta = 1$, $\beta = 2$, and $\beta = \infty$ is represented by graphs (a), (c), and (d). The graphs we have obtained at other parameter values are not significantly different than what would be obtained by interpolating these results.

Related work. Shirley & Wang [1992] have also compared BRDF and light source sampling techniques for the glossy highlights problem. They analyze a specific Phong-like BRDF and a specific light source sampling method, and derive an expression for when to switch from one to the other (as a function of the Phong exponent, and the solid angle occupied by the light source). Their methods work well, but they apply only to this particular BSDF and sampling technique. In contrast, our methods work for arbitrary BSDF's and sampling techniques, and can combine samples from any number of techniques.

9.3.2 The final gather problem

In this section we consider a simple test case motivated by multi-pass light transport algorithms. These algorithms typically compute an approximate solution using the finite element method, followed by one or more ray tracing passes to replace parts of the solution that are poorly approximated or missing. For example, some radiosity algorithms use a *local pass* or *final gather* to recompute the basis function coefficients more accurately.

We examine a variation called *per-pixel final gather*. The idea is to compute an approximate radiosity solution, and then use it to illuminate the visible surfaces during a ray tracing pass [Rushmeier 1988, Chen et al. 1991]. Essentially, this type of final gather is equivalent to ray tracing with many area light sources (one for each patch, or one for each link in a hierarchical solution). That is, we would like to evaluate the scattering equation (9.2) where L_{e} is given by the initial radiosity solution.

As with the glossy highlights example, there are two common sampling techniques. The brightest patches are typically reclassified as "light sources" [Chen et al. 1991], and are sampled using direct lighting techniques. For example, this might consist of choosing one sample for each light source patch, distributed according to the emitted power per unit area. The remaining patches are handling by sampling the BSDF at the point intersected by the viewing ray, and casting rays out into the scene. If any ray hits a light source patch, the contribution of that ray is set to zero (to avoid counting the light source patches twice). Within

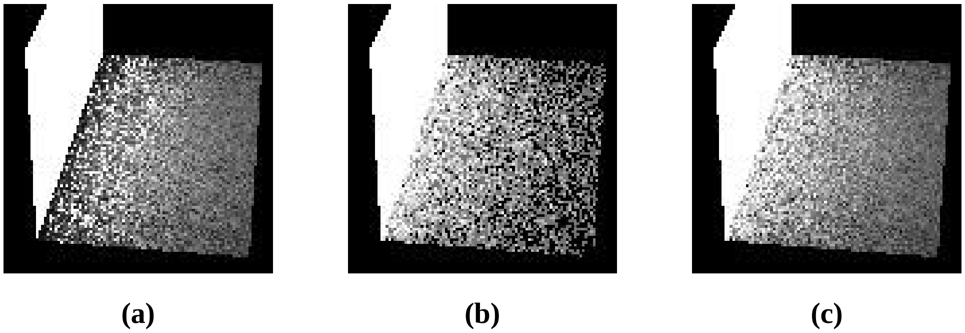

Figure 9.12: A simple test scene consisting of one area light source (i.e. a bright patch, in the radiosity context), and an adjacent diffuse surface. The images were computed by **(a)** sampling the light source according to emitted power, using $n_1 = 3$ samples per pixel, **(b)** sampling the BSDF with respect to the projected solid angle measure, using $n_2 = 6$ samples per pixel, and **(c)** a weighted combination of samples from (a) and (b) using the power heuristic with $\beta = 2$.

our framework for combining sampling techniques, this is clearly a partitioning of the integration domain into two regions.

Given some classification of patches into light sources and non-light sources, we consider alternative ways of combining the two types of samples. To test our combination strategies, we used the extremely simple test scene of Figure 9.12, which consists of a single area light source and an adjacent diffuse surface. Image (a) was computed by sampling the light source according to emitted power, while image (b) was computed by sampling the BSDF and casting rays out into the scene. Twice as many samples were taken in image (b) than (a); in practice this ratio would be substantially higher (i.e. the number of directional samples, compared to the number of samples for any one light source).

Notice that the sampling technique in Figure 9.12(a) does not work well for points near the light source, since this technique does not take into account the $1/r^2$ distance term of the scattering equation (9.2). On the other hand Figure 9.12(b) does not work well for points far away from the light source, where the light subtends a small solid angle. In Figure 9.12(c), the power heuristic is used to combine samples from (a) and (b). As expected, this method performs well at all distances. Although (c) uses more samples (the sum of (a) and (b)), this still is a valid comparison with the partitioning approach described above (which also uses

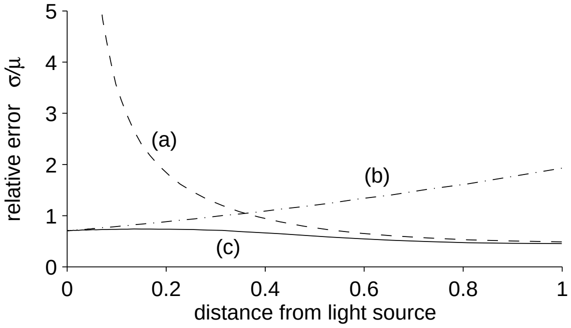

Figure 9.13: A plot of the relative error σ/μ, as a function of the distance from the light source. Three curves are shown, corresponding to the three images of Figure 9.12. The curves have been normalized to show the variance when $n_1 = 1$ and $n_2 = 2$ (the same ratio of samples used in Figure 9.12).

both kinds of samples).

Variance measurements for these experiments are plotted in Figure 9.13. There are three curves, corresponding to the three images of Figure 9.12. Each curve plots the relative error σ/μ as a function of the distance from the light source. Notice that the combined curve (c) always lies below the other two curves, indicating that both kinds of samples are being used effectively. Also, notice that unlike Figure 9.10, the variance curves do not approach zero at the extremes of the distance axis (not even as the distance d goes to infinity). This implies that neither of the given sampling techniques is an excellent match for the integrand, so that the balance, cutoff, power, and maximum heuristics all perform similarly on this problem. This is why we have only shown one graph, rather than four.

9.4 Discussion

There are several important issues that we have not yet discussed.

We start by considering how multiple importance sampling is related to the classical Monte Carlo techniques of importance sampling and stratified sampling. We show that it unifies and extends these ideas within a single sampling model. Next, we consider the problem of choosing the n_i, i.e. how to allocate a fixed number of samples among the given sampling techniques. We argue that this decision is not nearly as important as choosing the weighting functions appropriately. Finally, we discuss some special issues that arise in direct lighting problems.

9.4.1 Relationship to classical Monte Carlo techniques

Multiple importance sampling can be viewed as a generalization of both importance sampling and stratified sampling. It extends importance sampling to the case where more than one sampling technique is used, while it extends stratified sampling to the case where the strata are allowed to overlap each other. From the latter point of view, multiple importance sampling consists of taking one or more samples in each of n given regions Ω_i. These regions do not need to be disjoint; the only requirement is that their union must cover the portion of the domain where f is non-zero.

This generalization of stratified sampling is useful, especially when the integrand is a sum of several quantities. A good example in graphics is the BSDF, which is often written as a sum of diffuse, glossy, and specular components (for reflection and/or transmission). The process of taking one or more samples from each component is essentially a form of stratified sampling, where the strata overlap.

When stratified sampling is generalized in this way, however, there is more than one way to compute an unbiased estimate of the integral (since when two strata overlap, samples from either or both strata can be used). To address this, multiple importance sampling assigns an explicit representation to each possible unbiased estimator (as a set of weighting functions w_i). Furthermore it provides a reasonable way to select one of these estimators, by showing that certain estimators perform well compared to all the rest.

9.4.2 Allocation of samples among the techniques

In this section, we consider how to choose the number of samples that are taken using each technique p_i. We show that this decision is not as important as it might seem at first: no strategy is that much better than that of simply setting all the n_i equal.

To see this, suppose that a total of N samples will be taken, and that these samples must be allocated among the n sampling techniques. Let F be an estimator that allocates these samples in any way desired (provided that $\sum_i n_i = N$), and uses any weighting functions desired (provided that F is unbiased). On the other hand, let $\hat{F}$ be the estimator that takes an equal number of samples from each p_i, and combines them using the balance heuristic. Then it is straightforward to show that

$$V[\hat{F}] \;\leq\; n\, V[F] + \frac{n-1}{N}\, \mu^2$$

where as usual, $\mu = E[F]$ is the quantity to be estimated (see Theorem 9.5 in Appendix 9.A for a proof).

According to this result, changing the n_i can improve the variance by at most a factor of n, plus a small additive term. In contrast, a poor choice of the w_i can increase variance by an arbitrary amount. Thus, the sample allocation is not as important as choosing a good combination strategy.

Furthermore, the sample allocation is often controlled by other factors, so that the optimal sample allocation is irrelevant. For example, consider the glossy highlights problem. In a distribution ray tracer, the samples used to estimate the glossy highlights are also used for other purposes: e.g. the light source samples are used to estimate the diffuse shading of the surface, while the BSDF samples are used to compute glossy reflections of ordinary, non-light-source objects. Often these other purposes will dictate the number of samples taken, so that the sample allocation for the glossy highlights calculation cannot be chosen arbitrarily. On the other hand, by computing an appropriate weighted combination of the samples that need to be taken anyway, we can reduce the variance of the highlight calculation essentially for free.

Similarly, the sample allocation is also constrained in bidirectional path tracing. In this case, it is for efficiency reasons: it is more efficient to take one sample from all the techniques at once, rather than taking different numbers of samples using each strategy. (This will be discussed further in Chapter 10.)

9.4.3 Issues for direct lighting problems

The glossy highlights and final gather test cases are both examples of direct lighting problems. They differ only in the terms of the scattering equation that cause high variance: in the case of glossy highlights, it was the BSDF and the emission function L_{e}, while for the final gather problem it was the $1/r^2$ distance factor.

Although there are more sophisticated techniques for direct lighting that take into account more factors of the scattering equation [Shirley et al. 1996], it is still useful to combine several kinds of samples. There are several reasons for this. First, sophisticated sampling strategies are generally designed for a specific light source geometry (e.g. the light source must be a triangle or a sphere). Second, they are often expensive: for example, taking a sample may involve numerical inversion of a function. Third, none of these strategies is perfect: there are always some factors of the scattering equation that are not included in the approximation (e.g. virtually all direct lighting strategies do not consider the BSDF or visibility factors). Thus, in parts of the scene where these unconsidered factors are dominant, it can be more efficient to use a simpler technique such as sampling the BSDF. Thus, combining samples from two or more techniques can make direct lighting calculations more robust.

9.5 Conclusions and recommendations

As we have shown, multiple importance sampling can substantially reduce the variance of Monte Carlo rendering calculations. These techniques are practical, and the additional cost is small — less than 5% of the time in our tests was spent evaluating probabilities and weighting functions. There are also good theoretical reasons to use these methods, since we have shown strong bounds on their performance relative to all other combination strategies.

For most Monte Carlo problems, the balance heuristic is an excellent choice for a combination strategy: it has the best theoretical bounds, and is the simplest to implement. The additional variance term of $(1/\min_i n_i - 1/N)\,\mu^2$ is not an issue for integration problems of reasonable complexity, because it is unlikely that any of the given density functions p_i will be an excellent match for f. Under these circumstances, even the optimal combination F^* has considerable variance, so that the maximum improvement that can be obtained by using some other strategy instead of the balance heuristic is a small fraction of the total.

On the other hand, if it is possible that the given integral is a low-variance problem (i.e. one of the p_i is good match for f), then the power heuristic with $\beta = 2$ is an excellent choice. It performs similarly to the balance heuristic overall, but gives better results on low-variance problems (which is exactly the case where better performance is most noticeable). Direct lighting calculations are a good example of where this optimization is useful.

In effect, multiple importance sampling provides a new viewpoint on Monte Carlo integration. Unlike ordinary importance sampling, where the goal is to find a single “perfect” sampling technique, here the goal is to find a set of techniques that *cover* the important features of the integrand. It does not matter if there are a few bad sampling techniques as well — some effort will be wasted in sampling them, but the results will not be significantly affected. Thus, multiple importance sampling gives a recipe for making Monte Carlo software more reliable: whenever there is some situation that is not handled well, then we can simply add another sampling technique designed for that situation alone. We believe that there are many applications that could benefit from this approach, both in computer graphics and elsewhere.

Appendix 9.A Proofs

Proof of Theorem 9.2 (from p. 264). Let $F_{i,j}$ be the random variable

$$F_{i,j} \;=\; \frac{w_i(X_{i,j})\, f(X_{i,j})}{p_i(X_{i,j})}\,,$$

and let μ_i be its expected value

$$\begin{aligned} \mu_i &= E[F_{i,j}] \\ &= \int_\Omega w_i(x)\, f(x)\, d\mu(x) \end{aligned}$$

(which does not depend on j). We can then write the variance of F as

$$\begin{aligned} V[F] &= V\left[\sum_{i=1}^{n} \frac{1}{n_i} \sum_{j=1}^{n_i} F_{i,j}\right] \\ &= \sum_{i=1}^{n} \frac{1}{n_i^2} \sum_{j=1}^{n_i} V[F_{i,j}] \\ &= \left(\sum_{i=1}^{n} \frac{1}{n_i^2} \sum_{j=1}^{n_i} E[F_{i,j}^2]\right) - \left(\sum_{i=1}^{n} \frac{1}{n_i^2} \sum_{j=1}^{n_i} E[F_{i,j}]^2\right) \\ &= \left(\sum_{i=1}^{n} \frac{1}{n_i^2} \sum_{j=1}^{n_i} \int_\Omega \frac{w_i^2(x)\, f^2(x)}{p_i^2(x)}\, p_i(x)\, d\mu(x)\right) - \left(\sum_{i=1}^{n} \frac{1}{n_i^2}\, n_i\, \mu_i^2\right) \\ &= \left(\int_\Omega \sum_{i=1}^{n} \frac{w_i^2(x)\, f^2(x)}{n_i\, p_i(x)}\, d\mu(x)\right) - \left(\sum_{i=1}^{n} \frac{1}{n_i}\, \mu_i^2\right). \end{aligned} \tag{9.16}$$

Notice that there are no covariance terms, because the $X_{i,j}$ are sampled independently.

We will bound the two parenthesized expressions separately. To minimize the first expression

$$\int_\Omega \sum_{i=1}^{n} \frac{w_i^2(x)\, f^2(x)}{n_i\, p_i(x)}\, d\mu(x)\,, \tag{9.17}$$

it is sufficient to minimize the integrand at each point x separately. Noting that $f^2(x)$ is a constant and dropping x from our notation, we must minimize

$$\sum_{i=1}^{n} \frac{w_i^2}{n_i\, p_i}$$

subject to the condition $\sum_i w_i = 1$. Using the method of Lagrange multipliers, the minimum value is attained when all $n+1$ partial derivatives of the expression

$$\sum_i \frac{w_i^2}{n_i\,p_i} + \lambda \left(\sum_i w_i - 1 \right)$$

are zero. This yields n equations of the form $-2\,w_i \;=\; n_i\,p_i\,\lambda$, together with constraint $\sum_i w_i = 1$. The solution of these equations is

$$\hat{w}_i \;=\; \frac{n_i\,p_i}{\sum_k\,n_k\,p_k}$$

(the balance heuristic). Thus no other combination strategy can make the first variance term of (9.16) any smaller.

We now consider the second variance term of (9.16), namely

$$\sum_{i=1}^{n} \frac{1}{n_i}\,\mu_i^2\,.$$

We will prove an upper bound of $(1/\min_i n_i)\,\mu^2$ and a lower bound of $(1/\sum_i n_i)\,\mu^2$, such that these bounds hold for any functions w_i. (Recall that $\mu = E[F]$ is the quantity to be estimated.) Combining this with the previous result, we immediately obtain the theorem.

For the upper bound, we have

$$\sum_i \frac{1}{n_i}\,\mu_i^2 \;\le\; \frac{1}{\min_i n_i} \sum_i \mu_i^2 \;\le\; \frac{1}{\min_i n_i} \left(\sum_i \mu_i \right)^2 \;=\; \frac{1}{\min_i n_i}\,\mu^2\,,$$

where the second inequality holds because all the μ_i are non-negative.

For the lower bound, we minimize $\sum_i \mu_i^2/n_i$ subject to the constraint $\sum_i \mu_i \;=\; \mu$. Using the method of Lagrange multipliers, the minimum is attained when all $n+1$ partial derivatives of the expression

$$\sum_i \frac{\mu_i^2}{n_i} + \lambda \left(\sum_i \mu_i - \mu \right)$$

are zero. This yields $n+1$ equations whose solution is $\mu_i \;=\; (n_i/\sum_k n_k)\,\mu$, so that the minimum value of the second variance term of (9.16) is

$$\sum_i \frac{1}{n_i} \left(\frac{n_i}{\sum_k n_k}\,\mu \right)^2 \;=\; \frac{1}{\sum_k n_k}\,\mu^2$$

as desired. ∎

Proof of Theorem 9.3 (from p. 274). According to the arguments of the previous theorem, it is sufficient to prove a bound of the form

$$\sum_i \frac{w_i^2(x)\, f^2(x)}{n_i\, p_i(x)} \;\le\; c \sum_i \frac{\hat{w}_i^2(x)\, f^2(x)}{n_i\, p_i(x)}$$

at each point x, where the w_i are the weighting functions given by one of the heuristics of Theorem 9.3, and the $\hat{w}_i$ are given by the balance heuristic. Dropping the argument x, letting $q_i = n_i p_i$, and substituting the definition

$$\hat{w}_i = \frac{q_i}{\sum_k q_k}\,,$$

we must show that

$$\sum_i \frac{w_i^2}{q_i} \;\le\; c \sum_i \frac{1}{q_i} \left(\frac{q_i}{\sum_k q_k} \right)^2 \;=\; \frac{c}{\sum_k q_k}\,. \tag{9.18}$$

For the cutoff heuristic, we have

$$\begin{aligned} \sum_i \frac{w_i^2}{q_i} &= \sum_{i \mid q_i \ge \alpha\, q_{\max}} \frac{1}{q_i} \left(\frac{q_i}{\sum_{k \mid q_k \ge \alpha\, q_{\max}} q_k} \right)^2 \\ &= \frac{1}{\sum_{i \mid q_i \ge \alpha\, q_{\max}} q_i}\,. \end{aligned}$$

Thus according to (9.18), we must find a value of c such that

$$\begin{aligned} && \frac{1}{\sum_{i \mid q_i \ge \alpha\, q_{\max}} q_i} &\le \frac{c}{\sum_k q_k} \\ \Longleftrightarrow && c \sum_{i \mid q_i \ge \alpha\, q_{\max}} q_i &\ge \sum_k q_k \\ \Longleftrightarrow && (c-1) \sum_{i \mid q_i \ge \alpha\, q_{\max}} q_i &\ge \sum_k q_k - \sum_{i \mid q_i \ge \alpha\, q_{\max}} q_i \\ \Longleftrightarrow && c - 1 &\ge \frac{\sum_{i \mid q_i < \alpha\, q_{\max}} q_i}{\sum_{i \mid q_i \ge \alpha\, q_{\max}} q_i}\,. \end{aligned}$$

To find a value of c for which this is true, it is sufficient to find an upper bound for the right-hand side. Examining the numerator and denominator, we have

$$\frac{\sum_{i \mid q_i < \alpha\, q_{\max}} q_i}{\sum_{i \mid q_i \ge \alpha\, q_{\max}} q_i} \;\le\; \frac{(n-1)\, \alpha\, q_{\max}}{q_{\max}} \;=\; \alpha\, (n-1)\,.$$

Thus the variance claim is true whenever $c \ge 1 + \alpha\, (n-1)$, as desired.

Next, we consider the power heuristic with the exponent $\beta = 2$. Starting with the inequality

(9.18), we have

$$\sum_i \frac{w_i^2}{q_i} \;=\; \sum_i \frac{1}{q_i} \left(\frac{q_i^2}{\sum_k q_k^2} \right)^2 \;=\; \frac{\sum_i q_i^3}{\left(\sum_k q_k^2\right)^2} \, . \tag{9.19}$$

Thus we must find a value of c such that

$$\begin{array}{lrcl} & \dfrac{\sum_i q_i^3}{\left(\sum_k q_k^2\right)^2} & \leq & \dfrac{c}{\sum_k q_k} \\ \Longleftrightarrow & \left(\sum_i q_i\right) \left(\sum_i q_i^3\right) & \leq & c \left(\sum_k q_k^2\right)^2 \, . \end{array} \tag{9.20}$$

Notice that this inequality is unchanged if all the q_i are scaled by a constant factor. Thus without loss of generality we can assume that

$$\sum_i q_i^2 \;=\; \sum_i q_i \, , \tag{9.21}$$

so that our goal reduces to finding a value of c such that

$$c \;\geq\; \left(\sum_i q_i^3\right) \,/\, \left(\sum_i q_i^2\right) \, .$$

We proceed as before, by finding an upper bound for the right-hand side. Without loss of generality, let q_1 be the largest of the q_i. Observing that

$$\left(\sum_i q_i^3\right) \,/\, \left(\sum_i q_i^2\right) \;\leq\; \max_i q_i \;=\; q_1 \, ,$$

it is sufficient to find an upper bound for q_1. According to (9.21), we have

$$q_1^2 - q_1 \;=\; \sum_{i=2}^{n} q_i - q_i^2 \, .$$

Letting S denote the quantity on the right-hand side, we have $S \;\leq\; (1/4)\,(n{-}1)$, since the maximum value of $q_i - q_i^2$ is attained when $q_i = 1/2$. Thus using the quadratic formula, we have

$$\begin{array}{lrcl} & q_1^2 - q_1 & \leq & (1/4)\,(n-1) \\ \Longrightarrow & q_1 & \leq & (1/2)\,(1 + \sqrt{(-1)^2 + 4\,(1/4)\,(n-1)}) \\ & & = & (1/2)\,(1 + \sqrt{n}) \, . \end{array}$$

Thus, the original inequality (9.18) is true for any value of c larger than this.

For an exponent in the range $1 \leq \beta \leq \infty$, the argument is similar. We find that

$$\sum_i \frac{w_i^2}{q_i} \;=\; \left(\sum_i q_i^{2\beta-1}\right) / \left(\sum_k q_k^\beta\right)^2$$

(compare this with (9.19)), and we must find a value of c for which

$$\left(\sum_i q_i\right) \left(\sum_i q_i^{2\beta-1}\right) \;\le\; c \left(\sum_k q_k^\beta\right)^2$$

(compare with (9.20)). By scaling all the q_i by a constant factor, we can assume without loss of generality that

$$\sum_i q_i^\beta \;=\; \sum_i q_i \,, \tag{9.22}$$

so that we must find a value of c that satisfies

$$c \;\ge\; \frac{\sum_i q_i^{2\beta-1}}{\sum_i q_i^\beta} \,.$$

Letting q_1 be the largest of the q_i, a trivial upper bound for the right-hand side is $q_1^{\beta-1}$. Our strategy will be to find an upper bound for this quantity, in terms of β and n.

Defining

$$S \;=\; \sum_{i=2}^{n} q_i - q_i^\beta \tag{9.23}$$

and using the restriction (9.22), we have

$$\begin{aligned} & q_1^\beta - q_1 &=&\; S \\ \Longrightarrow\quad & q_1^{\beta-1} &=&\; 1 + S/q_1 \,. \end{aligned} \tag{9.24}$$

To find an upper bound for the right-hand side, we must find an upper bound for S, and a lower bound for q_1. For q_1, we have

$$\begin{aligned} & q_1^\beta &=&\; q_1 + S \\ \Longrightarrow\quad & q_1^\beta &\ge&\; S \\ \Longrightarrow\quad & q_1 &\ge&\; S^{1/\beta} \,, \end{aligned}$$

and inserting this in (9.24) yields

$$q_1^{\beta-1} \;\le\; 1 + S^{1-1/\beta} \,. \tag{9.25}$$

Now to find an upper bound for S, from (9.23) we have

$$S \;\le\; (n-1) \sup_{x\ge 0} (x - x^\beta) \,. \tag{9.26}$$

The maximum value of $f(x) = x - x^\beta$ occurs when $f'(x) = 0$, yielding

$$\begin{array}{rrcl} & 1 - \beta x^{\beta-1} & = & 0 \\ \Longrightarrow & x & = & (1/\beta)^{1/(\beta-1)} \,. \end{array}$$

Substituting this in (9.26), we obtain an upper bound for S:

$$\begin{aligned} S &\le (n-1)\left((1/\beta)^{1/(\beta-1)} - (1/\beta)^{\beta/(\beta-1)}\right) \\ &= (n-1)\,(1/\beta)^{1/(\beta-1)}\,(1 - 1/\beta)\,. \end{aligned}$$

Finally, we combine this with (9.25) to obtain an upper bound for $q_1^{\beta-1}$:

$$\begin{aligned} q_1^{\beta-1} &\le 1 + S^{1-1/\beta} \\ &\le 1 + \left[(n-1)\,(1/\beta)^{1/(\beta-1)}\,(1-1/\beta)\right]^{(\beta-1)/\beta} \\ &= 1 + (1/\beta)^{1/\beta}\,((n-1)(1-1/\beta))^{1-1/\beta} \end{aligned}$$

as desired.

Notice that for the case $\beta = 2$, this argument gives a bound of

$$c \;=\; (1/2)\,(2 + \sqrt{n-1})\,,$$

which is slightly larger than the bound of $c = (1/2)\,(1 + \sqrt{n})$ previously shown. ∎

Tightness of the bounds. For the cutoff heuristic, the constant c cannot be reduced for any value of α. (To see this, let $q_1 = 1$, and let $q_i = \alpha - \epsilon$ for all $i = 2, \ldots, n$, where $\epsilon > 0$ can be made as small as desired.)

For the power heuristic, the given bounds are tight when $\beta = 1$ and $\beta = \infty$ (corresponding to the balance and maximum heuristics respectively, and yielding the constants $c = 1$ and $c = n$. For other values of β, the bounds are not tight. However, they are not as loose as might be expected, considering the simplifications that were made to obtain them. For example, let $q_1 = 1 + \sqrt{n}$, and $q_i = 1$ for $i = 2, \ldots, n$. Substituting these values into the defining equation (9.20) for c, we obtain

$$c \;=\; (1/4)\,(3 + \sqrt{n})\,.$$

Thus, the bounds $c = (1/2)\,(1 + \sqrt{n})$ and $c = (1/2)\,(2 + \sqrt{n-1})$ proven above cannot be reduced by more than a factor of two.

Proof of Theorem 9.4 (from p. 276). The variance of F is

$$V[F] = E[F^2] - E[F]^2 \,.$$

Since $E[F]^2 = \mu^2$ is the same for all unbiased estimators, it is enough to show that the balance heuristic minimizes the second moment $E[F^2]$. We have

$$\begin{aligned} E[F^2] &= \sum_{i=1}^{n} c_i \int_\Omega \frac{w_i^2(x)\, f^2(x)}{c_i^2\, p_i^2(x)}\, p_i(x)\, d\mu(x) \\ &= \int_\Omega \sum_{i=1}^{n} \frac{w_i^2(x)\, f^2(x)}{c_i\, p_i(x)}\, d\mu(x) \,. \end{aligned}$$

Except for the substitution of c_i for n_i, this expression is identical to the second moment term (9.17) that was minimized in the proof of Theorem 9.2. Thus, the balance heuristic minimizes $E[F^2]$, and we are done. ∎

The following theorem concerns the allocation of samples among the given sampling techniques. Before stating it, we first rewrite the multi-sample estimator (9.4) to allow for the possibility that some n_i are zero:

$$F = \sum_{i=1}^{n} \sum_{j=1}^{n_i} \frac{w_i(X_{i,j})\, f(X_{i,j})}{n_i\, p_i(X_{i,j})} \,, \tag{9.27}$$

where $n_i \geq 0$ for all i. The possibility that $n_i = 0$ also requires a modification to condition (W2) for F to be unbiased:

(W2') $w_i(x) = 0$ whenever $n_i p_i(x) = 0$.

We now have the following theorem (which was informally summarized in Section 9.4.2):

Theorem 9.5. *Let f, p_1, …, p_n, and the total number of samples N be given, where $N = kn$ for some integer k. Let F be any unbiased estimator of the form (9.27), and let $\hat{F}$ be the corresponding estimator that uses the weighting functions*

$$\hat{w}_i(x) = \frac{n_i\, p_i(x)}{\sum_k n_k\, p_k(x)}$$

(the balance heuristic), and takes an equal number of samples from each p_i. Then

$$V[\hat{F}] \;\leq\; n\, V[F] + \frac{n-1}{N}\, \mu^2 \,,$$

where $\mu = E[F]$ is the quantity to be estimated.

Proof. Given any unbiased estimator F, let F^+ be the estimator that uses the same weighting functions F ($w_i^+ = w_i$), but takes an equal number of samples using each sampling technique ($n_i^+ = N/n$). We will show that $V[F^+] \le n\, V[F]$. Starting with equation (9.16) for $V[F]$, we have

$$\begin{aligned}
V[F] &= \int_\Omega \sum_{i=1}^n \frac{w_i^2(x)\, f^2(x)}{n_i\, p_i(x)}\, d\mu(x) \;-\; \sum_{i=1}^n \frac{1}{n_i}\, \mu_i^2 \\
&= \sum_{i=1}^n \frac{1}{n_i} \left(\int_\Omega \frac{w_i^2(x)\, f^2(x)}{p_i(x)}\, d\mu(x) \;-\; \mu_i^2 \right) \\
&\ge \sum_{i=1}^n \frac{1}{N} \left(\int_\Omega \frac{w_i^2(x)\, f^2(x)}{p_i(x)}\, d\mu(x) \;-\; \mu_i^2 \right) \\
&= \frac{1}{n} \sum_{i=1}^n \frac{1}{N/n} \left(\int_\Omega \frac{w_i^2(x)\, f^2(x)}{p_i(x)}\, d\mu(x) \;-\; \mu_i^2 \right) \\
&= \frac{1}{n}\, V[F^+]\,.
\end{aligned}$$

We now compare the variance of F^+ to the variance of $\hat{F}$. These two estimators take the same number of samples from each p_i, so that we can apply Theorem 9.2:

$$\begin{aligned}
V[\hat{F}] &\le V[F^+] \;+\; \left(\frac{1}{\min_i n_i^+} - \frac{1}{\sum_i n_i^+} \right) \mu^2 \\
&\le n\, V[F] \;+\; \left(\frac{1}{N/n} - \frac{1}{N} \right) \mu^2 \\
&= n\, V[F] + \frac{n-1}{N}\, \mu^2\,. \quad \blacksquare
\end{aligned}$$